ELSEVIER

Journal of Controlled Release 37 (1995) 199–214

journal of controlled release

Prediction of solvent removal profile and effect on properties for peptide-loaded PLGA microspheres prepared by solvent extraction/evaporation method

Wen-I Li [a], Kimberly W. Anderson [b], Rahul C. Mehta [1,c], Patrick P. DeLuca [c,*]

[a] *Department of Chemical Engineering, Pennsylvania State University, University Park, PA 16802, USA*

[b] *Department of Chemical Engineering, University of Kentucky, Lexington, KY 40506, USA*

[c] *College of Pharmacy, University of Kentucky, Lexington, KY 40536, USA*

Received 3 November 1994; accepted 5 May 1995

Abstract

Using a predictive mathematical model, several important extrinsic process variables were varied to simulate the process dynamics of microsphere formation. These included the composition profile in the dispersed phase, the solvent concentration profile in the continuous phase and the solvent removal profile in the dispersed phase. By superimposing the composition profile in the dispersed phase with the phase transition boundary, the progression of phase transition in microsphere formation can be evaluated. Low dispersed phase/continuous phase ratio, high continuous phase-addition rate, high temperature, high heating rate and high initial polymer concentration in the dispersed phase contributed to enhanced solvent removal. The higher solvent removal led to a heterogeneous composition distribution in the dispersed phase and the early cross-over of the gelation point (viscous boundary) of the periphery region which initiates the onset of solidification in this region. These phenomena resulted in an increasing pore size, lower surface area, denser periphery, higher residual solvent and slower drug release. In addition, the progress toward the glassy boundary may also play a major role in the ultimate solvent residual. Slow solvent removal gave rise to a homogenous distribution of the components in the dispersed phase due to the delay of hardening. The extrinsic manageable parameters could be varied during microsphere formation to obtain the desired rate of solvent removal as well as the desired microsphere properties. The mathematical model was used to simulate such conditions to facilitate the experimental design for the desired microsphere properties.

Keywords: Microsphere; Solvent removal; Controlled release; Pore formation

1. Introduction

Biodegradable polymeric microspheric matrices have high potential as peptide drug carriers, since they meet the specific delivery requirements of controlled release, peptide protection and specific targeting [1]. Although various methods and a variety of polymers are available to prepare microspheres very few processes are available for the preparation of microspheres of controlled porosity. Matrices of variable porosity facilitate modulation of drug release. Porous microspheres are also essential to deliver high molecular weight substances which cannot diffuse out of a non-porous matrix and to deliver substances which have

* Corresponding author.

[1] Present address: Isis Pharmaceuticals, Carlsbad, CA 92008, USA.

SSDI 0168-3659(95)00076-3

high affinity for polymer and are not released unless the matrix is eroding. Matrix porosity is also of significance in polymeric carriers which deliver drugs, at least in part, by erosion. Polymer degradation can be controlled by altering the porosity of the matrix and hence control the rate and extent of drug release.

Porous polylactide/glycolide (PLGA) microspheres incorporated with polypeptide have been prepared using a solvent extraction/evaporation method. Preliminary studies have shown that by changing the process variables, microspheres of different porosity/surface areas could be obtained [2]. Parameters important to impart porosity are not well defined and there is a need to understand the process of pore formation so that the preparation of porous microspheres can be controlled, monitored and reproduced.

In a previous publication, a mathematical model for microsphere formation using a solvent extraction/evaporation method was developed and tested using the experimental data of salmon calcitonin, (sCT),-loaded PLGA microspheres [3]. In this paper the mass transfer model coupled with phase transition boundary will be used to analyze the progression of microsphere formation. Additionally, the mechanism of microsphere formation and the effects of process variables on solvent removal and microsphere hardening (or solidification) were investigated. The results were related to the microsphere properties, such as pore structure, surface area, drug distribution/load and release.

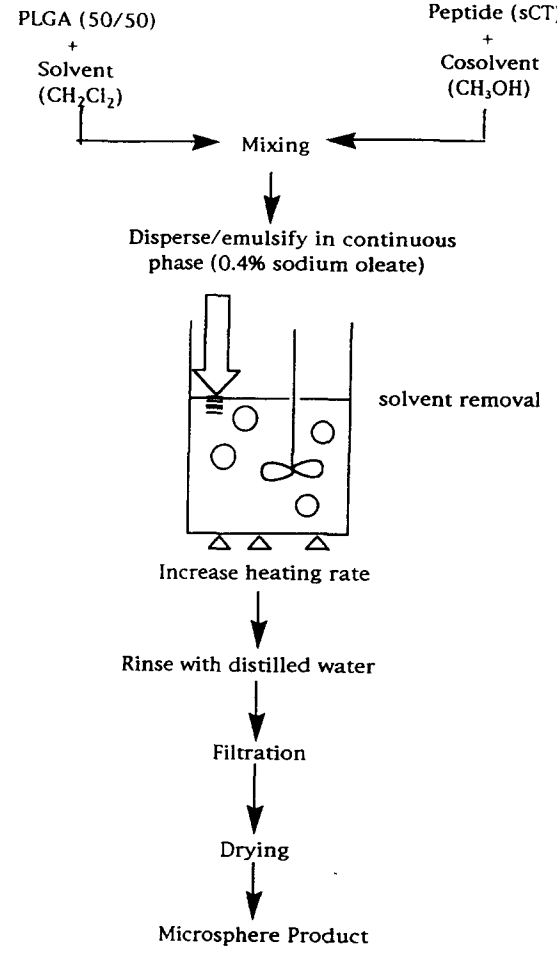

Fig. 1. Schematic diagram of manufacturing process for microspheres loaded with peptide.

2. Theory

Microsphere formation as illustrated in Fig. 1 can be separated into three stages; (1) droplet formation, (2) solvent removal/solidification and (3) refinement/drying. During droplet formation, most of cosolvent (CH_3OH) and a portion of the solvent(CH_2Cl_2) were extracted by the continuous phase (CP); where, subsequently, the CH_2Cl_2 evaporated at the CP surface/air interface. The diffusion of solvent in the peripheral layers of the droplets make the cortical part semisolid; and with the aid of the surface active agent, the droplets were stabilized.

The residual solvent in the droplets at this stage is a precursor for the final properties of the microspheres, especially, the porosity. The subsequent solvent removal stage can be carried out using volume gradient (VG) methods.

The principle of the VG method is the gradual removal of the dispersed phase (DP) solvents by the addition of fresh CP thereby continuing the gradual extraction of the DP solvents. This process undergoes two subsequent phase separations; liquid-liquid and then, solid-liquid separation.

The schematic diagram for the phase separation is shown in Fig. 2. The miscibility of a peptide such as sCT in a PLGA/CH_2Cl_2 solution is very limited. Therefore, the peptide can be near saturation or even in suspension in the dispersed phase. Peptide-polymer association is facilitated in the solution form, while peptide encapsulation is promoted in the suspension

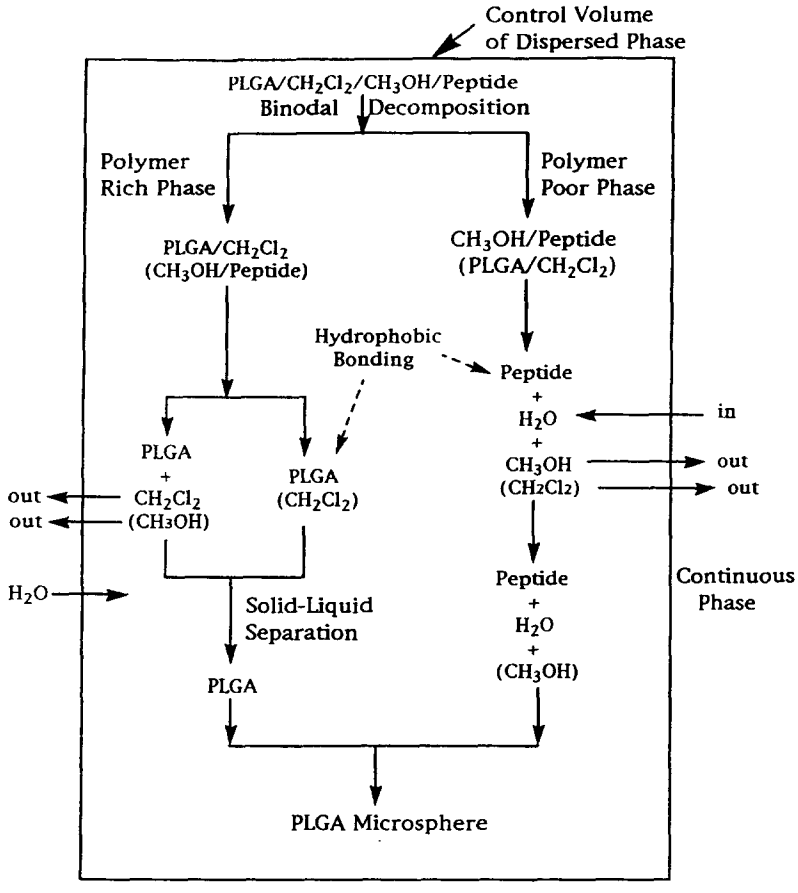

Fig. 2. Schematic diagram of the phase separations during microsphere formation.

form. The treatment in this research will be to effect the former recognizing that during the process some free peptide in solution will precipitate and be encapsulated. With the subsequent diffusion of solvent/cosolvent into the CP, the composition of the polymer solution reaches the binodal boundary. A ternary phase diagram for the solvent/cosolvent/polymer system is shown in Fig. 3. The binodal points are thermodynamically unstable. The composition along the binodal curve will be decomposed into two phases: polymer rich and polymer poor phases. The liquid-liquid separation due to binodal decomposition has been studied extensively in the formation of polymeric membranes [4–6].

The polymer rich phase is made up of PLGA and CH_2Cl_2 with small amounts of CH_3OH/peptide. Most of the CH_3OH is then separated from the polymer rich phase to form a polymer poor phase containing most of the peptide. Peptide association with the polymer occurs in the liquid-liquid phases.

This non-PLGA phase serves as an important medium for cosolvent in the DP to exchange with water in the CP. The other path for water entering the DP (droplet) is through the polymer rich phase. However, this path has limitations due to the low solubility of water in CH_2Cl_2 and PLGA. More cosolvent such as CH_3OH helps the uptake of water into the DP through this path. The comparison of the water flow with other component fluxes is shown in Fig. 4. The more water entrapped inside the microsphere, the more porous the microspheres will be. If the microspheres remain soft or the distribution of solvent in the polymer is high and homogeneous, more water can diffuse into the non-PLGA phase to create more water pockets (Fig. 2). If the shell or cortical layer has already been solidified, the structure is more fixed and less water may be

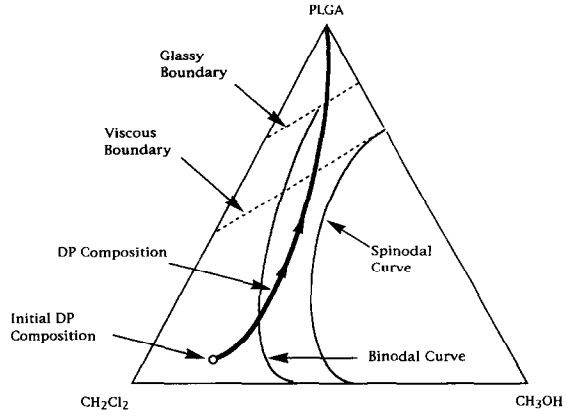

Fig. 3. Ternary phase diagram for the microdroplet in the dispersed phase.

allowed to diffuse into the non-PLGA phase. Actually, solidification and water-uptake are compromising processes. In some cases, solidification dominates the process while in others water-uptake dominates the process.

The peptide plays an important role in the pore formation of the microsphere. Depending upon the type of entrapment, the peptide may serve different roles. In the first type, the peptide can be entrapped inside the polymer without interconnection with other peptide molecules or without access to the microsphere surface or the CP. This type is called dead-end segment. The peptide entrapped as a dead-end segment inside the DP absorbs CH_3OH during binodal decomposition or may retain water from the polymer rich route. Both H_2O and CH_3OH are porosity precursors.

For the second type of entrapped peptide, the peptide has access to the polymer surface. The peptide can associate with PLGA through hydrophobic bonding. Therefore, the peptide can exhibit amphipathic properties; dissolved in water and adsorbed onto PLGA. This type of behavior provides the major source for pore creation. The interaction, especially, hydrophobic bonding, between PLGA and sCT has been described [7].

At the same time, the polymer rich phase undergoes solution-gel separation. When the DP solvent diffuses into the CP, it leaves the polymer-rich phase more concentrated and more viscous. The viscosity of the

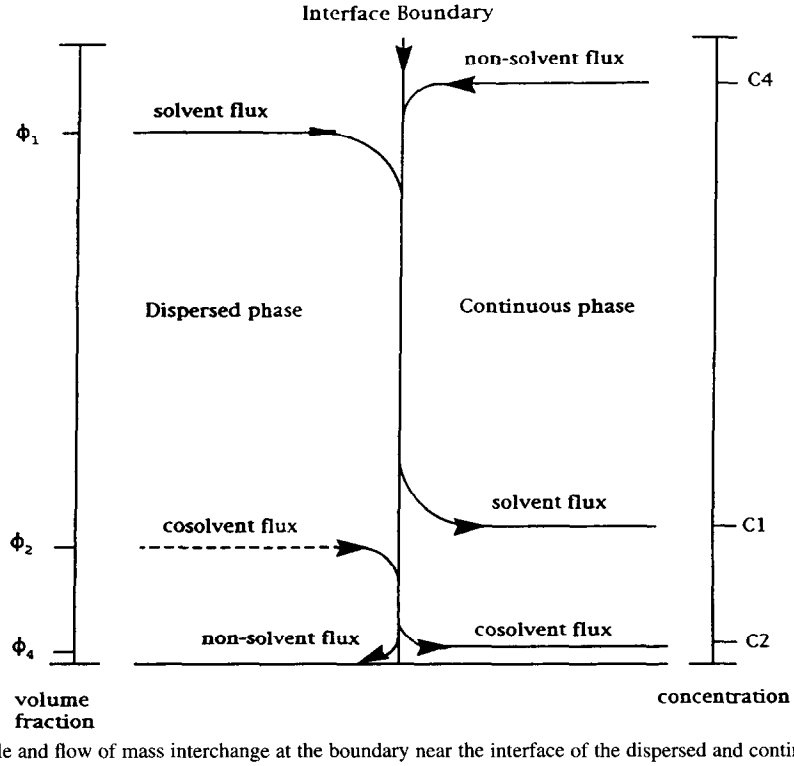

Fig. 4. Conceptual profile and flow of mass interchange at the boundary near the interface of the dispersed and continuous phases. ϕ_1, ϕ_2 and ϕ_4 represent the volume fraction of solvent, cosolvent and nonsolvent, respectively. C_1, C_2 and C_4 represent solvent, cosolvent and nonsolvent, respectively.

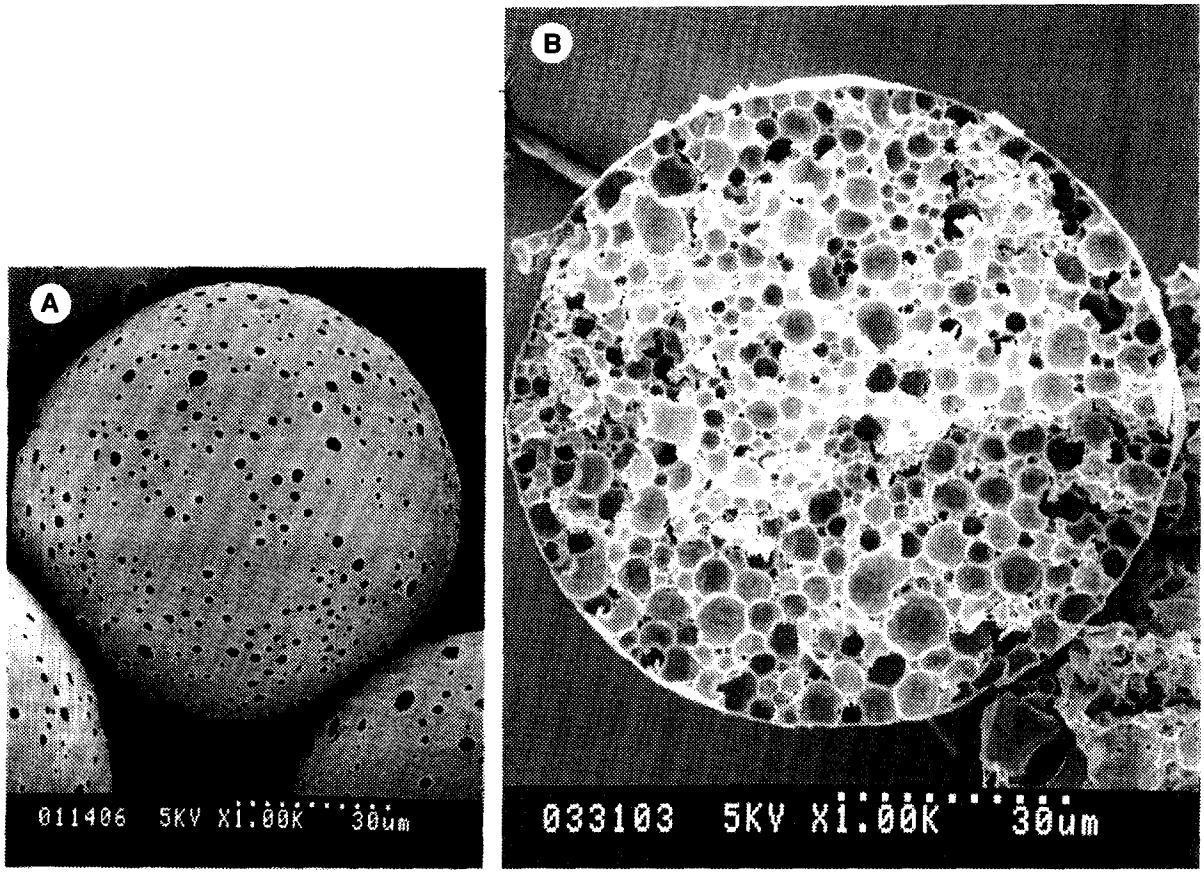

Fig. 5. SEM photomicrograph of sCT microspheres prepared by volume gradient method: (a) surface morphology, (b) cross-sectional view of internal structure [2,10].

microsphere at this stage is in the low Reynolds flow region, $R_e \sim 10^{-12}$, according to Amundson et al. [8]. Consequently, the mass transfer of solvent through this concentrated region will decrease exponentially. The polymer rich region at the viscous boundary will undergo phase transition; converting from the sol state to the gel state. This can be verified from the measurement of the gelation temperature of the concentrated polymer solution. After hardening, the gel-like region is separated from the rest of the liquid state polymer-rich region.

The further removal of solvent from the gelation region induces glass transition in the polymer rich phase. At this stage, the microspheres are in the glassy state, and the solidification is complete. The solid-gel separation increases the difficulty of solvent passing through the solidified region.

Water uptake accelerates the formation of pores within microspheres; however, rapid solidification hinders the uniform formation of pores. Both factors are interrelated in generating the internal pore structure. The internal pore structure and external morphology of microspheres formed by the CP-dilution and replacement techniques are shown by the SEMs in Fig. 5. The pore formation mechanism described above for microspheres apparently gives rise to the unique pore structure for microspheres.

3. Methodology

The mathematical model for the microsphere formation developed in the previous publication [3] was used to simulate the process kinetics of microsphere

formation. In the process kinetics, the composition profile of each component in the DP, the solvent removal profile in the DP and the concentration of solvent in the CP were calculated. The composition profiles in the DP were further superimposed on the phase transition diagram and the resulting diagram was used to evaluate the progression of the phase transition in the DP. The analysis of composition profile and phase transition were related to the experimental microsphere properties and used to predict the microsphere properties.

The mathematical model for microsphere formation was divided into three parts, the governing equation in the DP, the governing equation in the CP and the coupled equation for the radius and volume change of the DP. The governing equation in the DP expressed the change of the volume fraction of DP component with respect to time and space as follows:

$$\frac{D(\phi_i/\phi_3)}{Dt}=\frac{-1}{\bar{r}(t)\phi_3}\nabla_\xi\cdot\left[\frac{D_i}{RT}\nabla_\xi\mu_i\right]$$
$$-\left[\frac{v_3}{\bar{r}(t)}-\frac{\xi}{\bar{r}(t)}\frac{d\bar{r}(t)}{dt}\right]\cdot\nabla_\xi(\phi_i/\phi_3)\quad i=1,2,4 \qquad (1)$$

where ϕ_i represent the volume fraction of component i in the DP, $i=1$ solvent, $i=2$ cosolvent, $i=3$ polymer and $i=4$ nonsolvent, respectively. $\xi=r/\bar{r}(t)$ is the normalized radial position, r is any position in the microdroplet/microspheres, $\bar{r}(t)$ is the radius of microdroplet/microspheres at any time. v_3 is the velocity of polymer. D_i is the diffusion coefficient of solvent in polymer. μ_i is the chemical potential of component in the DP. Based on the results of simplified case section in previous publication [3], currently, a pseudo-binary system was adapted for the purpose of calculation; this is based on the cosolvent outflow and nonsolvent influx in the DP were almost completed at early stage. In such a case the i in the equation can be set as i = 1. Therefore, the effect of cosolvent and nonsolvent on the solvent chemical potential is assumed small, and the solvent chemical potential can be represented as:

$$\frac{\Delta\mu_1}{RT}=\ln(\phi_1)\beta\phi_3+(1+\chi_{13}\phi_3)(1-\phi_1) \qquad (2)$$

where χ_{13} represents the interaction of polymer and solvent. β is the ratio of the molar volume of solvent and polymer.

The solution of Eq. 1 can provide the information of the volume fraction of DP composition at any time and position inside the microsphere. The governing equation in the DP is subject to several system constraints such as initial and boundary conditions. The initial condition is

$$\phi_i(\xi,0)=\phi_i^0 \quad i=1,2,4 \qquad (3)$$

Boundary condition 1: the center of microspheres, $\xi=0$,

$$J_1(0,t)=0 \qquad (4)$$

Boundary condition 2: the surface of microspheres, $\xi=1.0$,

$$\phi_1(1.0,t)=qC_1^e \qquad (5)$$

where $J_1(0,t)$ is the volume flux at $\xi=0.0$. q is the partition coefficient of solvent in the CP and DP. C_1^e is the equilibrium concentration of solvent at the DP/CP interface. The governing equation in the DP is also coupled to the governing equation in the CP and the change rate of the radius and volume of microspheres.

The governing equation in the CP represents the concentration profile of solvent in the CP with respect to time. The solvent concentration profile in the CP is expressed as:

$$\frac{dC_1}{dt}=\frac{3.0(R_{DC})}{(1+\dot{V}t/V_0)}K_{x1}(C_1^e-C_1)\frac{\bar{r}(t)^2}{\bar{r}(0)^3}-\frac{(K_{y1}+\dot{V})}{V_T}C_1 \qquad (6)$$

where C_1 is the solvent concentration in the CP. R_{DC} is the volume ratio of the D/C which is an abbreviated form of DP/CP, K_{x1} is the mass transfer coefficient of solvent in the interface between DP and CP, V_0 is the initial volume of the DP. K_{y1} is the solvent evaporation constant and V_T is the total volume of the CP. The initial condition of solvent concentration in the CP was assumed to be zero. This equation also exhibits the extraction capability and evaporation extent of the CP.

The coupled equations used to calculate the rate of change of the radius and volume of the microdroplet in the DP were developed previously [3].

$$\frac{d\bar{r}(t)}{dt}=J_1(1,t)+J_2(1,t)+J_4(1,t) \qquad (7)$$

and

$$\frac{dY}{dt} = 3.0K_{x1}(C_1^s - C_1)\frac{\bar{r}(t)^2}{\bar{r}(0)^3} \quad (8)$$

where J_1, J_2 and J_4 represent the volume flux of solvent, cosolvent/nonsolvent flux. Y is the fraction change of the DP volume. The influx of nonsolvent and outflux of cosolvent can be assumed almost complete in the very early stage. Therefore, the volume flux of cosolvent and nonsolvent were considered as zero when the solvent removal process began. According to this concept, Eq. 7 was used to derive the solvent removal profile [3].

$$X = \frac{(Y + \phi_1^0 - 1.0)}{\phi_1^0} \times 100\% \quad (9)$$

where X represents the remaining percentage of solvent in the DP (X = present amount/initial amount × 100%). 1.0 represents the initial volume fraction of solvent in the DP.

As described in the preceding paper [3], the DP can be presented in three physical states; solution, gel and glassy. There are two important phase transitions. Viscous boundary, which is designated as the transition from the solution to gel state, and glassy boundary, which expresses the transition from gel to glassy state. At 25°C, the viscous boundary for the CH_2Cl_2-PLGA mixture was calculated as 0.41 volume fraction of CH_2Cl_2 and the glassy boundary was calculated at 0.1 volume fraction of CH_2Cl_2.

To simulate the microsphere formation process, it was necessary to input two process variables, intrinsic and extrinsic variables. The intrinsic process variables are the physico-chemical properties of the microsphere manufacturing system. These parameters are fixed when microsphere formation system is selected. On the other hand, the extrinsic process variables are adjustable during the formation process. The intrinsic variables for the PLGA microsphere process are shown in Table 1.

3.1. The extrinsic process variables

The extrinsic variables were usually used as adjusting parameters in the simulation. The tested model was employed in the simulation. In the simulation, the solvent removal profile, DP composition profile and solvent concentration profile in the CP were calculated by adjusting the extrinsic variables. These variables included D/C ratio, CP-dilution rate, temperature, temperature gradient, and DP composition. The adjusted ranges for each of the extrinsic variables are as follows:

Table 1
Summary of physico-chemical properties for mass transfer system

	Parameter	Components	Value	Unit
D_{14}	diffusion coefficient	CH_2Cl_2-H_2O	1.07×10^{-9}	m^2/s
K_{y1}	evaporation constant	CP-CH_2Cl_2-air	3.4×10^{-4}	1/s
D_{13}	frictional coefficient	CH_2Cl_2-PLGA	$2.0\times10^{-(8.0+4.9\phi_3)}$	m^2/s
χ_{13}	interaction parameter	CH_2Cl_2-PLGA	0.26	dimensionless

1. For D/C ratio effect, 1/10, 1/20, 1/25, 1/50, 1/100 or 1/200 ratios were used. Operational conditions were initial 500 ml CP volume and temperature of 15°C for 10 min followed by the addition of 3.8 ml CP/min at 25°C for the remainder of the process.
2. CP-addition rate: 0, 5 or 10 ml/min, starting with 500 ml CP. Operational conditions were D/C ratio 1/25, initial temperature of 15°C for 10 min followed by 25°C for the remainder of the process.
3. Temperature: 5°C, 15°C, 25°C or 35°C (kept constant throughout the process time). Operational conditions were initial 500 ml CP volume with 3.8 ml/min CP-addition rate and D/C ratio 1/25.
4. Heating rate: 0, 0.4 or 1.0°C/min. Operational conditions were D/C ratio 1/25, initial 500 ml CP volume with 3.8 ml/min CP-addition rate and initial temperature 15°C.
5. Volume fraction of solvent in the DP, 0.75, 0.90 or 0.95. Operational conditions were D/C ratio 1/25, initial 500 ml CP volume with 3.8 ml/min CP-addition rate and initial temperature 15°C for 10 min followed by 25°C for the rest of process.

The preparation process of sCT loaded PLGA microspheres has been described [2]. The microsphere properties at some of the above simulated conditions were obtained from the results of the sCT project. These included surface area, pore size, particle size, cross-section views of the microspheres, residual solvent and release profile.

4. Results and discussion

The effects of D/C ratio, CP-addition rate, temperature and initial DP composition on the solvent removal profile in the DP and solvent concentration in the CP were presented as follows.

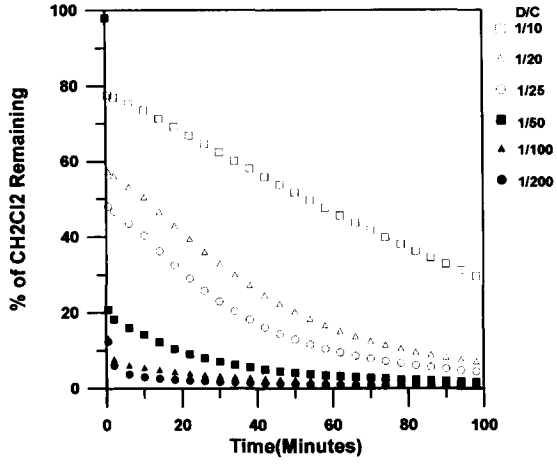

Fig. 6. Effects of D/C ratio on the removal of CH_2Cl_2 in the DP. *y*-axis is the percentage remaining of initial CH_2Cl_2 amount in the DP. The process temperature was initially 15°C for 10 min, then 25°C. The initial CP volume 500 ml with a CP-addition rate of 3.8 ml/min.

4.1. Effects of D/C ratio

Solvent removal

By solving Eqs. 1–9 simultaneously, the solvent removal profile can be predicted. Fig. 6 and Fig. 7 show the solvent removal profiles in the DP, and solvent concentration in the CP, respectively, at D/C ratios ranging from 1/10 to 1/200. From Fig. 6, the higher D/C ratio 1/10 showed very slow solvent removal, and within 100 min, there was still about 30% of initial CH_2Cl_2 amount left in the DP, while D/C ratios of 1/20 and 1/25 exhibited higher solvent removal rates. Almost 92% of initial CH_2Cl_2 was removed from the DP at near 80 and 60 min, respectively. From the concentration profile of CH_2Cl_2 in the CP, (Fig. 7) at a D/C ratio 1/10 the CH_2Cl_2 concentrations remained almost constant, while at D/C ratios of 1/20 and 1/25, the solvent concentration in the CP decreased with time. The low solvent concentration in the CP offers a better sink condition for solvent to be transferred into the CP. Within 40 seconds, 90% of the initial solvent amount in the DP was removed at D/C ratios of 1/100 and 1/200 (Fig. 6). An extremely low concentration of solvent in the CP provides a good concentration driving force for solvent removal (Fig. 7). The treat-

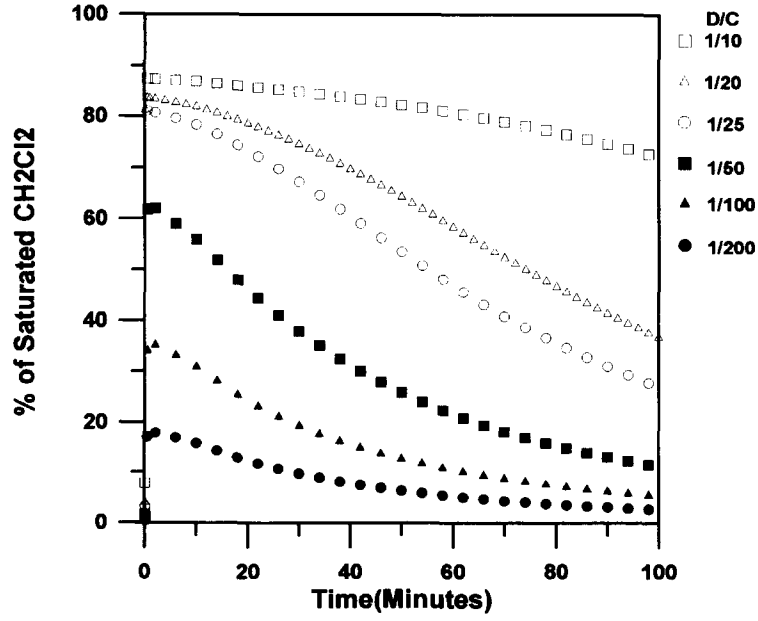

Fig. 7. Effect of D/C ratio on the concentration profiles of CH_2Cl_2 in the CP. The process temperature was 15°C for 10 min, then 25°C. The initial CP volume was 500 ml with a CP-addition rate of 3.8 ml/min.

ments illustrated by these two figures can be used to assess the kinetics of microsphere formation within a short time frame.

Solvent volume fraction in the DP

The solvent volume fractions throughout the DP in the course of microsphere formation are shown in Fig. 8a–f for all the D/C ratios. For the high ratios (1/10–1/25), the volume fraction of solvent in the microsphere will be uniformly distributed; there are no concentration gradients at the interior of the microspheres at any given time. For the low ratios from 1/50 to 1/200, the volume fraction of solvent inside the microsphere was unevenly distributed. The volume fraction near the interface between the CP and DP (cortical layer) was lower than that in the interior portion. The fast mass transfer induced by better sink conditions was the cause of such a phenomena. For D/C 1/100, the volume fraction of the cortical portion of the microsphere has already decreased to the level in the viscous boundary within 10 seconds of process time. In this sense, the outer layer of the microsphere becomes viscous first.

An early crossing of the viscous boundary caused several effects for microspheres prepared at lower D/C ratio (1/100). A viscous microsphere not only inhibits the movement of the active agent but also slows down the diffusion of low molecular weight molecules such as the solvent and nonsolvent. The porosity creator, water, has less of a chance to enter the microsphere. As mentioned in the mechanism section, the water solubility in CH_2Cl_2 is low; therefore, entering the polymer rich phase by inter-exchanging diffusion between CH_3OH and water is difficult. Preferably, water moves into the microsphere through the peptide or polymer poor phase. This phase is a more favorable environment for water, since CH_3OH is miscible with water and peptide (sCT) dissolves in water. The early hardening of the cortical layer and the interior hinders the movement of the peptide toward the periphery. Also, for the loading of 5% (w/w) peptide in polymer, the early distribution of peptide at the surface is not so extensive, and peptide at the surface can be extracted by the CP due to the high CP volume at lower D/C ratio such as 1/100. Therefore, in the periphery, the microspheres exhibit a denser polymer structure with few voids. The dense layer deters the mass transfer of water. Meanwhile, the early rapid interchange of H_2O and CH_2Cl_2/CH_3OH by extraction causes the drastic phase separation in the metastable state, which results in a coarser pore structure. The further mass transfer mainly consists of the diffusion of residual CH_2Cl_2 and CH_3OH out of the DP.

The structure of the microspheres prepared at lower D/C ratio (1/100) has been evaluated by TEM and surface area measurement (Fig. 9a). In the TEM, the cross-section view of microspheres exhibited substantial pores in the microsphere interior. The pore size was large with the average being ~ 12.5 μm. In addition, the outer layer of the microsphere was thick and dense, and the pores showed less interconnection. The surface area of microspheres was 2.94 m^2/g as measured by the krypton gas adsorption method.

For high D/C ratios, the solvent composition inside the microsphere is high and evenly distributed as shown in Fig. 8a–c. The peptide (sCT) has more of a chance to move around to pick out water and the CH_3OH pocket created by liquid-liquid separation can be replaced by water. Also, the less viscous microdroplets allows peptide to absorb water and swell. As evident from the SEM photomicrograph shown in Fig. 9b this space becomes void after drying. For the D/C ratio, 1/25, a smaller pore size with average diameter near 3.5 μm, more interconnection between pores and a very thin-layer resulted.

The structural differences of microspheres prepared at different D/C ratios caused variations in other microsphere properties such as final residual solvent and drug release profile. Therefore, at high D/C ratio, the peptide loading did not significantly decrease compared with that at low D/C ratio. For low D/C ratio, under the viscous layer condition, the peptide or active agent will be easily entrapped inside the microspheres, and the viscous layer hinders the movement of peptide or active agent into the CP. Therefore, the peptide will be more evenly distributed inside the microsphere.

The residual solvent of microspheres prepared at various D/C ratios are shown in Table 2. The high D/C ratio gave rise to lower residual solvent, <10 ppm, while the low D/C ratio ended up with higher residual solvent, 762 ppm. The residual solvent in the polymeric matrix must be below a toxic level for parenteral use. In the case of CH_2Cl_2, $<0.1\%$ or 1000 ppm should be the limit considering microspheres are administered in mg quantities.

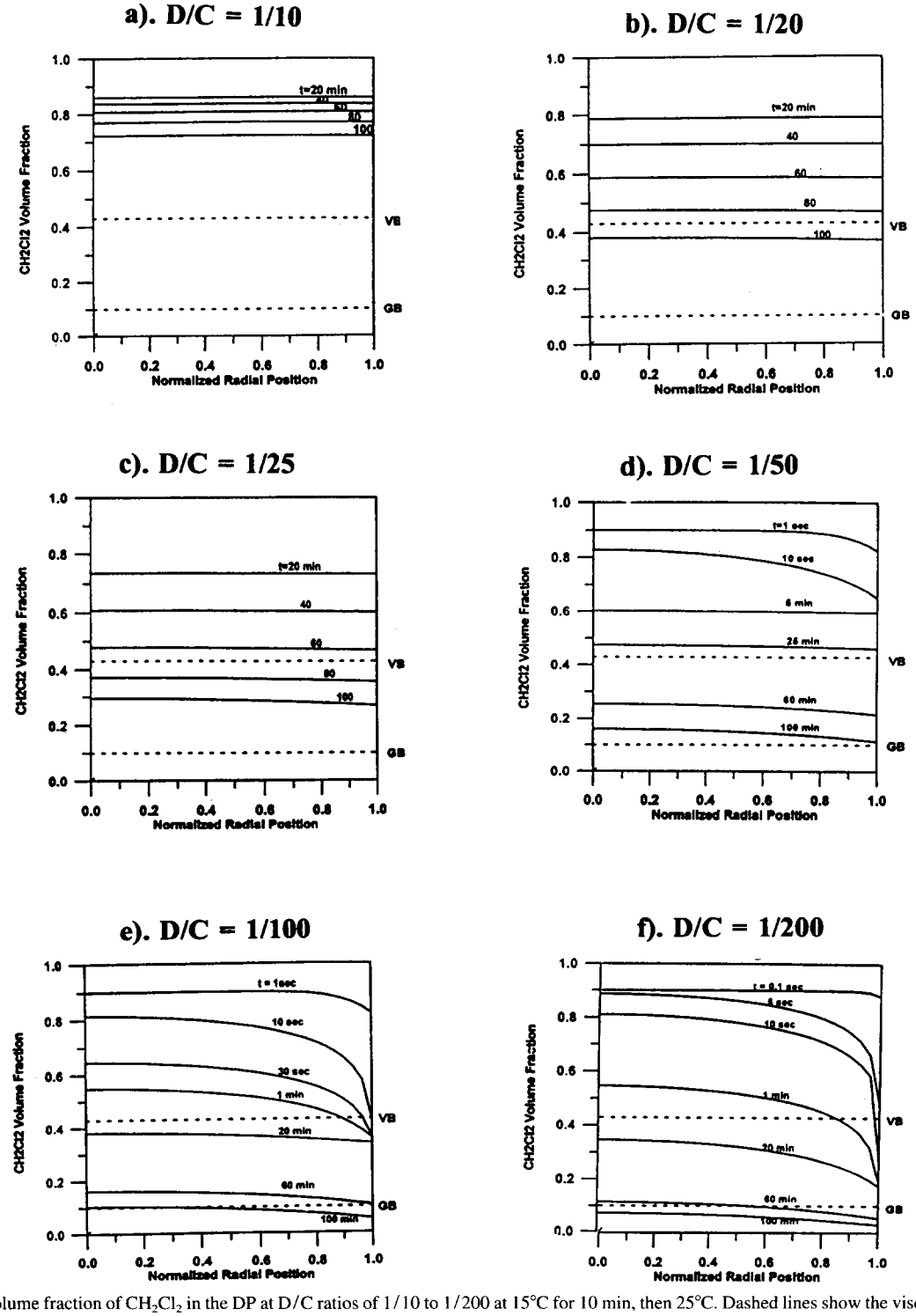

Fig. 8. Volume fraction of CH_2Cl_2 in the DP at D/C ratios of 1/10 to 1/200 at 15°C for 10 min, then 25°C. Dashed lines show the viscous (VB) and glassy (GB) boundaries. Normalized radial position, $\xi = r(t)/\bar{r}(t)$, is the radial position divided by the outside radius of the microspheres.

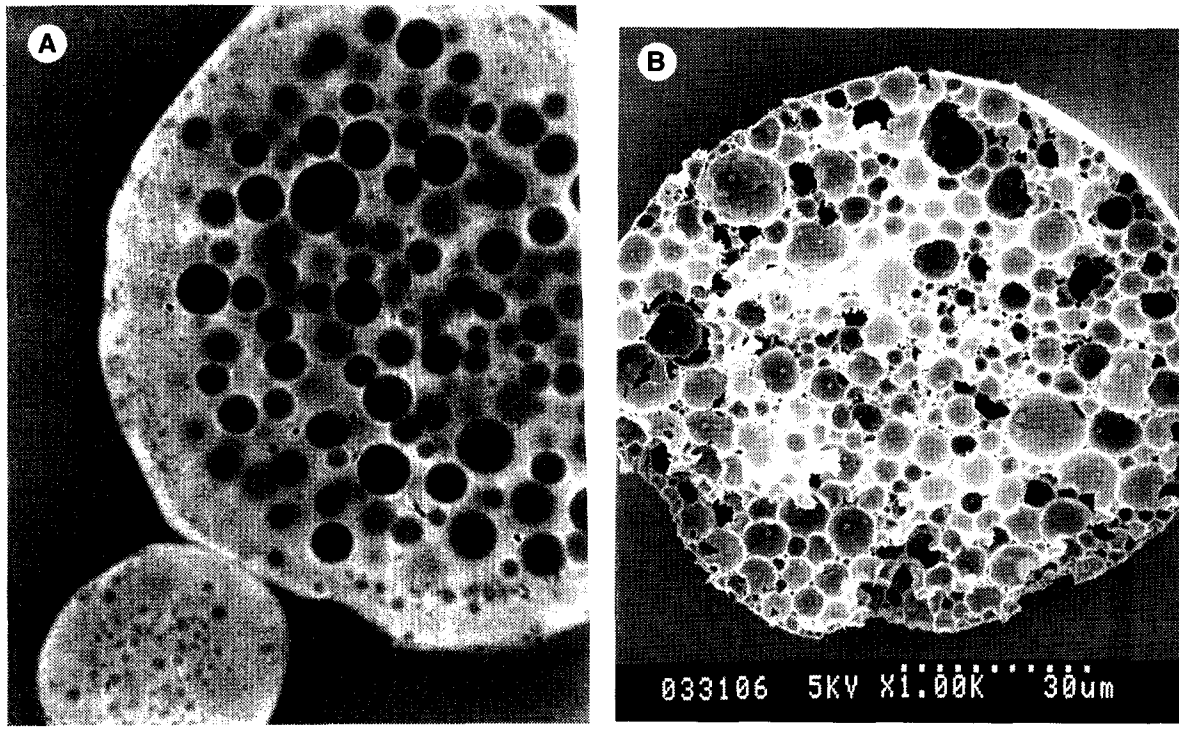

Fig. 9. Photomicrograph showing pore structure of sCT/PLGA microspheres prepared at D/C ratio: (a) 1/100, (b) 1/25 [2,11].

Table 2
Microsphere properties prepared at various D/C ratios (data from [2,10])

	D/C ratio			
	1/10	1/20	1/25	1/100
sCT loading (%)	3.4	3.08	3.4	3.4
Bulk density (g/ml)	0.05	0.09	0.09	–
Release	fast	fast	fast	slow
Solvent residual (ppm)	<10	<10	<10	762

Table 3
Drug release of sCT/PLGA microspheres prepared at high and low D/C ratios (data from [10,11])

	D/C ratio	
	1/25	1/100
In vitro release(%) (1 h)	28	0
In vivo release	days 0, 1, 3, 4	day 7

Note: whether the peptide released in vivo is determined by the detected serum level of peptide during daily analysis.

The rationale for the different residual solvent amounts in microspheres can be explained. At low D/C ratio, the early onset of solidification of the periphery of the microspheres and occurrence of a thick/dense skin layer, not only make the microspheres harder, but also promote liquid-solid separation. The mass transfer in this region is extremely slow, since the polymer chains are close together in the glassy state; thus the diffusion of solvent is more difficult, thereby entrapping it in the interior. For the high D/C case, the even solvent distribution, thin skin-layer and more interconnection between the pores facilitated the removal of the residual solvent during microsphere solidification.

The release of peptide (sCT) from PLGA microspheres prepared at D/C ratios of 1/25 and 1/100 are shown in Table 3 for in-vitro and in-vivo study. The release of peptide (sCT) was faster in the high D/C ratios from 1/10 to 1/25. This phenomenon can be rationalized by the high distribution of peptide in the periphery, more interconnection between pores and a very thin skin layer in the microspheres. Collectively, these factors facilitate the peptide release. For low D/C ratio, 1/100, the less peptide near periphery, a thick

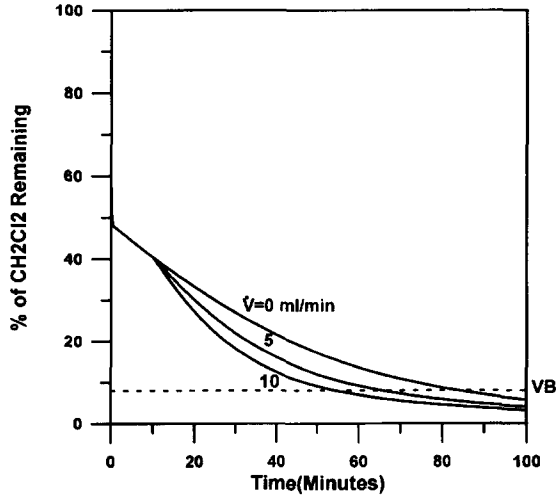

Fig. 10. Effect of CP-addition rate on the CH_2Cl_2 removal in the DP. Starting CP volume was 500 ml and 15°C for 10 min, then 25°C. Dashed lines represent the viscous boundary.

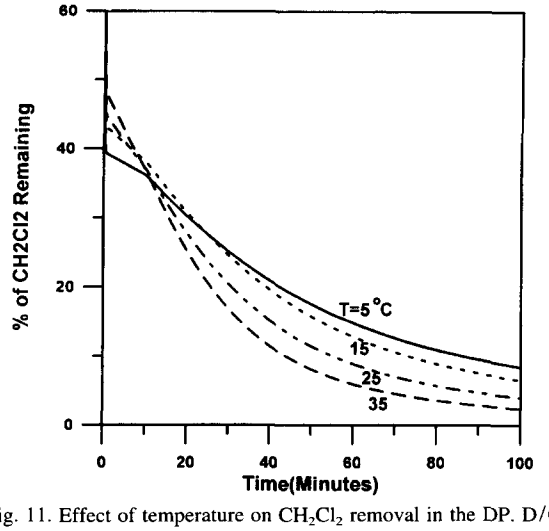

Fig. 11. Effect of temperature on CH_2Cl_2 removal in the DP. D/C ratio was 1/25. Starting CP volume was 500 ml with a CP-addition rate of 3.8 ml/min.

and dense skin layer, and less interconnection between pores hinders the diffusional release and retards the erosion of the matrix. This further slows down release by the erosion mechanism.

4.2. *Effects of CP-addition rate*

The effect of CP-addition rate on the solvent removal is shown in Fig. 10. The solvent removal without adding CP was slower; the time to reach the gelation point (viscous region) was around 80 min. With the CP-addition, the time to reach the viscous boundary with 92% of solvent in the DP having been removed was about of 60 min. Altering the CP-addition rate resulted in different pore structures; the higher CP-addition, the larger the pore size [2].

4.3. *Solvent removal at different temperature*

The solvent removal profiles for the different temperatures are shown in Fig. 11. The temperature was kept constant throughout the process. The initial extraction of solvent was highest at 5°C due to the higher solubility of CH_2Cl_2 at this temperature. The lower temperature offers a better sink condition for solvent removal, but also causes a lower evaporation rate due to lower mass transfer. Following the initial removal, solvent removal was higher at 15°C, 25°C and 35°C due to higher evaporation. At 35°C the viscous boundary will be reached first. The lower solubility of CH_2Cl_2 in the CP at the higher temperature is compensated for by the high evaporation rate.

The effect of heating rate on solvent removal is shown in Fig. 12. The heating rate in going from 15°C to 35°C at heating rates of 0.5 and 1.0°C per min did not have a substantial effect on the solvent removal.

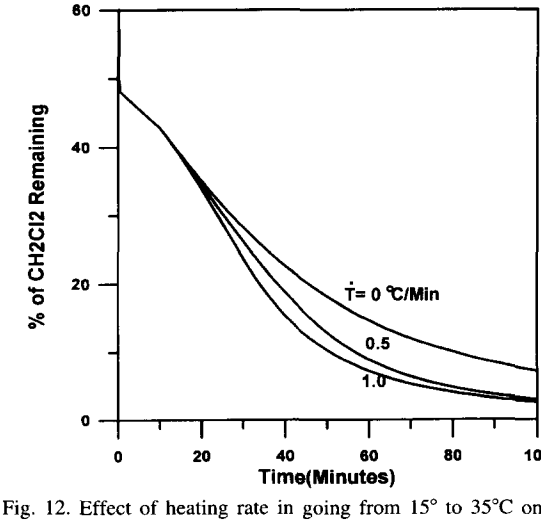

Fig. 12. Effect of heating rate in going from 15° to 35°C on the removal profile of CH_2Cl_2 in the DP. 0°C/min indicates maintaining the initial temperature at 15°C.

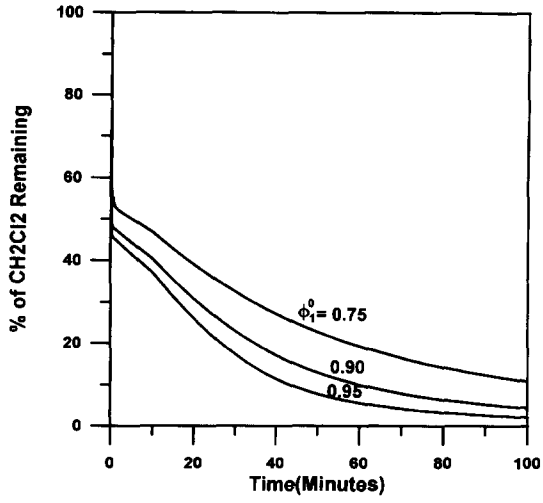

Fig. 13. Effect of solvent/ppolymer fraction on the removal of CH_2Cl_2 from the DP.

4.4. The effects of initial DP composition on solvent removal

To evaluate the effects of solvent/polymer concentration on the solvent removal, three solvent volume fractions, 0.75, 0.70 and 0.95 were used and the results are shown in Fig. 13. Using a D/C ratio of 1/25, the higher solvent concentration showed faster solvent removal due to the higher solvent concentration in the CP. On the other hand, with the low solvent concentration case, the solvent removal was slower due to the lower evaporation and lower solvent concentration in the CP.

The volume fraction of solvent with respect to the normalized radial position is plotted in Fig. 14. The lower solvent fraction (high polymer concentration) case showed more uneven distribution of solvent composition. The low solvent volume in the periphery region led to a homogeneous distribution of drug. For cisplatin/PLA microspheres [9], for which SEM photomicrographs are shown in Fig. 15, the preparation at low polymer concentration, 1 g PLA in 12.6 g CH_2Cl_2, produced uneven drug distribution, while at high polymer concentration, 1 g PLA in 8.4 g CH_2Cl_2, a more homogeneous drug distribution occurred.

As the polymer concentrates in the periphery, the active agent is hindered from moving into the CP while at same time solvent is entrapped inside. Therefore, a high residual solvent has been reported for high polymer concentration cases. Different DP composition

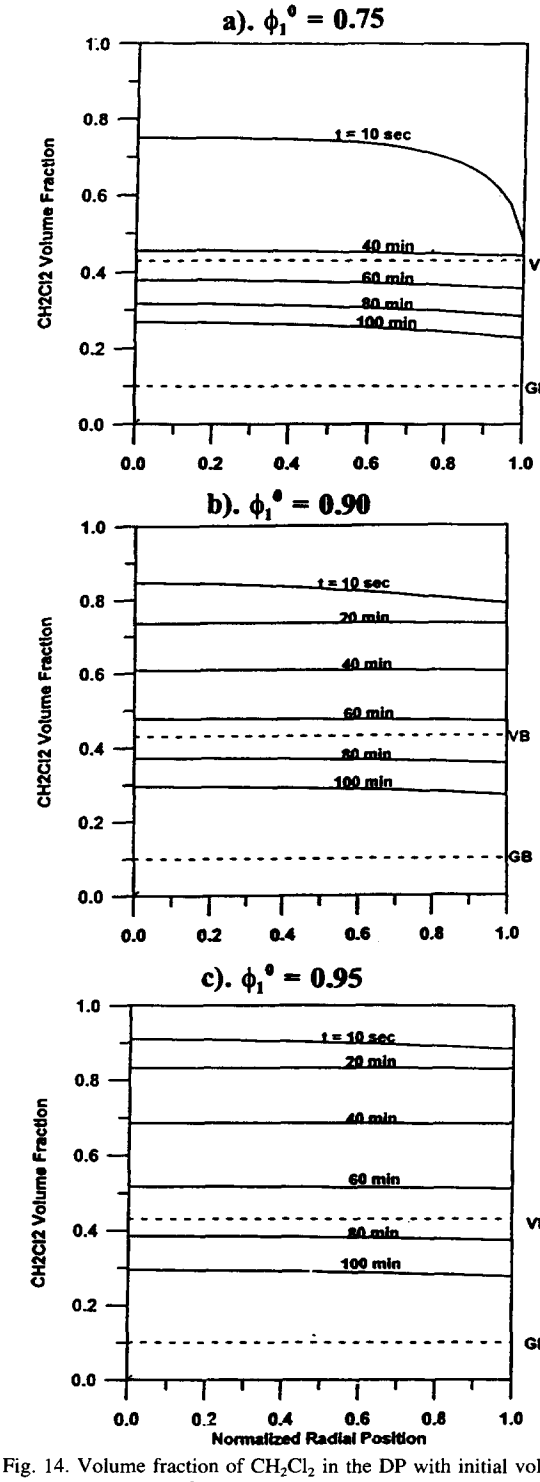

Fig. 14. Volume fraction of CH_2Cl_2 in the DP with initial volume fraction of CH_2Cl_2: ϕ_1^0 = (a) 0.75, (b) 0.90, (c) 0.95. Dashed lines are viscous boundary (VB) and glassy boundary (GB). Normalized radial position, $\xi = r(t)/\bar{r}(t)$, is the radial position divided by the outside radius of the microspheres.

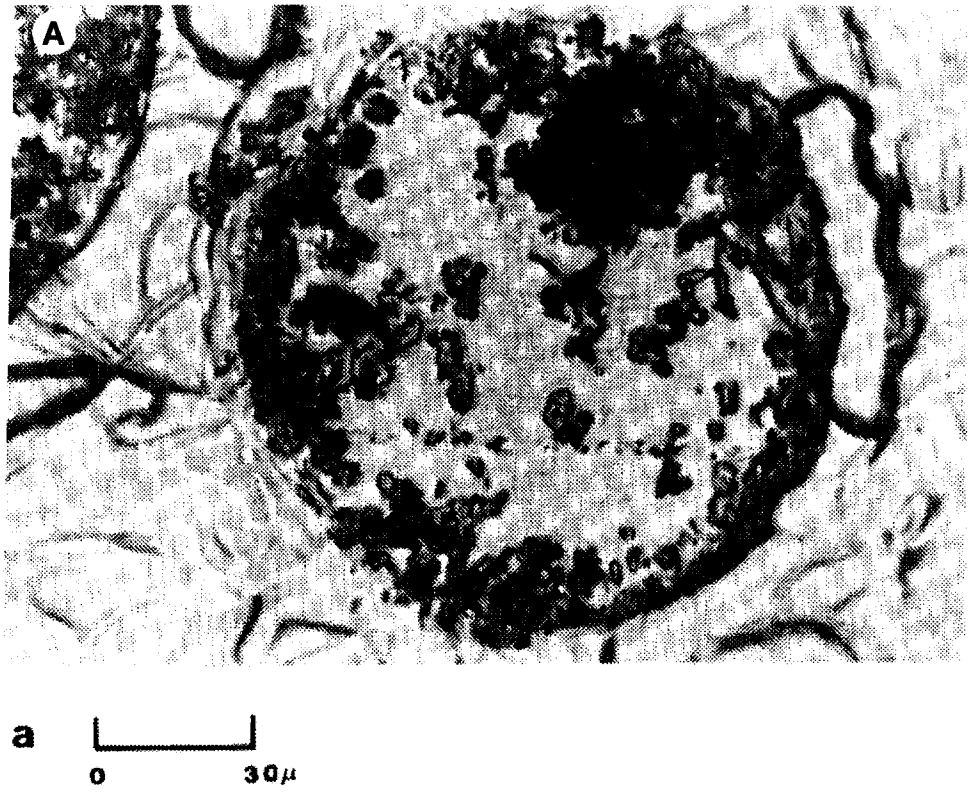

Fig. 15. Cross-sectional view of cisplatin/polylactide microspheres with: (a) 1 g of polymer in 12.6 ml CH_2Cl_2; (b) 1 g of polymer in 8.4 ml CH_2Cl_2 (from [9]).

results in different solvent removal and composition profiles in the course of microsphere formation. Although volume fractions of polymer and solvent of 0.1 and 0.9 are commonly chosen, compositions other than these would also give desired microsphere properties.

5. Conclusion

During the preparation of peptide-loaded polymeric microspheres, the multicomponent mass transfer, the interaction between components and the thermodynamics (phase separation) of the system are closely related. Specifically, the progression of phase transition (solidification) plays a major role in the resulting microsphere properties. This was verified by the predictive model and experimental data. Using the model, the process kinetics, namely solvent removal profile and DP composition profile, can be predicted and by the incorporation of phase transition boundary into the DP composition profile, the effects of extrinsic variables such as D/C ratio and initial DP composition on the progression of phase transition in the DP were evaluated. The difference in hardening resulted in different microsphere properties such as pore size, surface area, solvent residual and drug release as evident by the experimental data.

A low D/C ratio resulted in faster solvent removal. This was attributed to an uneven distribution in the droplet with concentrated and viscous periphery, and the time to reach the viscous and glassy boundaries was shorter. This resulted in lower porosity, higher drug loading and higher residual solvent. High D/C ratio caused lower solvent removal and longer time for the DP composition to reach the viscous (gelation) and glassy boundaries. Consequently, higher porosity, lower peptide loading, and lower residual solvent occurred in the resulting microsphere product.

Temperature also had a significant influence on solvent removal. At 5°C, solvent was initially removed more rapidly, due to high solubility of methylene chloride in the CP. Then, the solvent removal became sluggish due to the low evaporation capability as compared with 15, 25 and 35°C. Overall, the higher temperatures, reached the viscous boundary earlier than that of 5°C despite the higher solubility at 5°C.

The initial DP composition also influenced the solvent removal and resulting microsphere properties. A concentrated polymer solution in the DP resulted in higher solvent removal and rapid hardening of the periphery of the microspheres. Consequently, the drug loading was higher, porosity lower and residual solvent higher.

The methodology established can be used to analyze the process kinetics and dynamics of microsphere formation and by varying the extrinsic process variables, useful predictions of the process and microsphere properties can be made.

Acknowledgements

The authors gratefully acknowledge the numerous constructive comments of Dr. B.C. Thanoo. Partial support for this work was provided by an NSF Grant and an award from Marion Dow Co.

References

[1] A. Supersaxo, J.H. Kou, P. Teitelbaum and R. Maskiewicz, Preformed porous microspheres for controlled and pulsed release of macromolecules, J. Control. Release 23 (1993) 157–164.

[2] R. Jeyanthi, B.C. Thanoo, R.C. Mehta and P.P. DeLuca, Effect of solvent removal technique on the matrix characteristics of peptide-loaded PLGA microsphere, J. Control. Release (1996) in press.

[3] W.-I Li, K.W. Anderson and P.P. DeLuca, Kinetic and thermodynamic modeling of the formation of polymeric microspheres using solvent extraction/evaporation method, J. Control. Release 00 (1995) 00–00.

[4] C. Cohen, G.B. Tanny and S. Prager, Diffusion-Controlled formation of porous structures in ternary systems, J. Polym. Sci. Polym. Phys. Ed. 17, (1979) 477–489.

[5] S. Li, C. Jiang and Y. Zhang, The investigation of solution thermodynamics for the polysulfone-DMAC-water system, Desalination 62 (1987) 79–88.

[6] K. Kimmerle and H. Strathmann, Analysis of the structure-determining process of phase inversion membranes, Desalination 79 (1990) 283–302.

[7] T.L. Tsai, Dissertation, Study of peptide-polymer interaction and its implication in controlled drug delivery, University of Kentucky, Lexington, KY, April 1994.

[8] K.R. Amundson, D.W. Bousfield and D.S. Soong, Rheology of microsphere formation and refinement, J. Appl. Phys. 59 (1986) 2306–2312.

[9] G. Vert Spenlehauer, J. Benoit, F. Chabot and M. Veilard, J. Control. Release 7 (1989) 217–229.

[10] R.C. Mehta, R. Jeyanthi, S. Calis, B.C. Thanoo, K.W. Burton and P.P. DeLuca, Biodegradable microsphere as depot system for parenteral delivery of peptide drugs, J. Control. Release 29 (1994) 375–384.

[11] R. Jeyanthi, S. Calis, C. Mehta and P.P. DeLuca, Correlation of matrix properties and initial release behavior of calcitonin PLGA-microspheres, Pharm. Res. 10 (1993) S-277.